The Intelligent Merging Unit: Error Correction by Dynamic State Estimation

Miguel Jiménez Aparicio
Term Project - ECE 6323: Power System Protection
Georgia Institute of Technology
Atlanta, United States of America
maparicio6@gatech.edu

***Abstract*—Power system protection depends on relays that are able to detect a fault when occurs and then take the necessary actions to ensure the system safety. These relays use instrumentation channels that reduce the magnitude of the voltage and current on the line before taking the measurements. However, there are some known effects in the transformer of the instrumentation channel that could lead to a wrong calculation of the real magnitude of the primary current, and therefore mislead the relay about the decision it should take. In order to solve this problem, a Graphical User Interface (GUI) has been developed with the objective of performing a state estimation of the system and detect whether if a fault has occurred or not. The GUI has been programmed to read data in COMTRADE format and display useful information that helps the user to understand the behavior of the system.**

***Index Terms*—State estimation, fault detection, current instrumentation channel, Graphical User Interface (GUI), COMTRADE format.**

I. Introduction

The correct operation of the grid ultimately depends on the control systems that regulate voltages and power flows through the lines, and on the protection systems that guarantee the safety of the system when a fault occurs. Protection elements use measurements from different types of units and devices to decide whether a fault has occurred and the line should be tripped or not. This decision implies a huge economical cost if is taken wrongly and there is no fault on the line, but it is worse, even risking human lives, if there is a fault and the protection devices don't actuate. Therefore, it is very important to ensure the correctness of the measurements that may motivate those decisions.

From a technical point of view, the instrumentation channels need to transform the high voltage and current waveforms that are present on the transmission lines onto a lower magnitude that a device such a relay can handle. Typically, a current transformer (CT) performs this task. However, during a fault, the extremely high currents may provoke that, due to the core saturation, the waveforms seen at the secondary side are not a true reflection of the current that goes through the line - which is called the primary current. This information is critical as the eventual decision which is performed by the relay will depend on it, as it has been mentioned before.

In order to solve this, and get the real magnitude of the current through the line, this paper proposes an state estimation approach to obtain the primary current from the measurements of the secondary current given by a CT. Once this estimation is performed, the results are analyzed using statistical methods. If the estimation gives a result that varies considerably from what would be reasonable for that particular moment, the algorithm will determine that there is a fault in the system.

II. Problem Formulation

Modern protection devices take samples of continuous waveforms, typically voltages, as the inputs for their calculations. Therefore, the available measurements of the secondary current of the current transformer, which are going to be used for the state estimation, are actually the voltage drop through a burden resistor. In Figure 1, it is possible to appreciate the schematic of a current transformer. The primary current, i_p, goes through the phase conductor. This current produces a magnetic flux that induces a current, i_s, in the secondary winding, and it goes through a twisted pair of copper conductors. Part of this current finally goes through a resistor, the burden resistor, producing a voltage drop, *Vout*, that is proportional to the current that goes through it. This voltage is measured by the measuring device using an Analog to Digital converter.

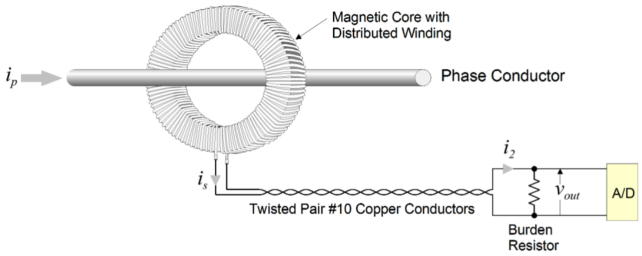

Fig. 1. Current instrumentation channel schematic

However, the state estimation requires a more accurate model of the instrumentation channel that includes all the impedances and losses in the wire, and that takes in account the model of the current transformer and the physics behind the magnetic flux. In Figure 2, the equivalent circuit of the current instruction channel is shown. This model is the same as the one proposed in [1], which is the documentation used as reference for this paper.

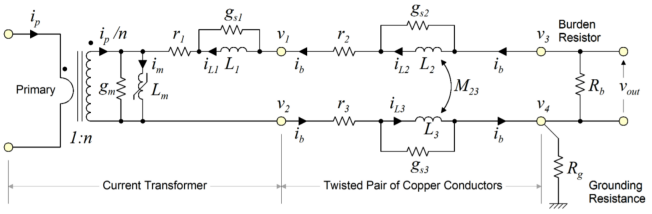

Fig. 2. Current instrumentation channel equivalent model

The model is defined in terms of the state variables, which include voltages and currents in different parts of the circuit, the magnetic flux and some non-linear combinations of it. This set of four non-linear combinations of λ(t), represented as y_i(t), are used to ensure that the model equations don't have an order greater than 2. There are 15 state variables in total. The state vector x is:

$$[v_1(t)\ v_2(t)\ v_3(t)\ v_4(t)\ e(t)\ \lambda(t)\ y_1(t)\ y_2(t)\ y_3(t)\ y_4(t)\ i_p(t)\ i_m(t)\ i_{L1}(t)\ i_{L2}(t)\ i_{L3}(t)]$$

The other parameters that appear in the model are included in the Appendix.

III. Solution Methodology

The developed solution has several steps: first, it is necessary to derive the mathematical model of the system measurements; second, it is necessary to perform the state estimation based on those measurements; finally, the estimation has to be validated using the Chi-Square test before taking any decision. An user interface, that will be introduced in the last section, has been developed with the purpose of facilitating the analysis of the results.

A. Measurements

For the project, a total of 21 measurements are considered, as it is suggested in [1]. Those measurements are actual, virtual derived and pseudo measurements, as it is detailed next.

1) Actual measurements: There is only one magnitude that it is actually measured, which is the voltage across the burden resistor. It is expressed are:

$$V_{out}(t) = v_3(t) - v_4(t) \tag{1}$$

2) Virtual measurements: This type of measurements are not magnitudes that are actually measured, instead they are derived from the usage of physical laws in different parts of the circuit. The following virtual measurements are derived:

- KCL at node 0 yields:

$$0 = -g_m e(t) - i_m(t) + \frac{1}{n} i_p(t) + i_{L_1}(t) + g_{s1} L_1 \frac{\mathrm{d}i_{L_1}(t)}{\mathrm{d}t} \tag{2}$$

- KCL at node 1 yields:

$$0 = g_m e(t) + i_m(t) - \frac{1}{n} i_p(t) - i_{L_2}(t) - g_{s2}(L_2 \frac{\mathrm{d}i_{L_2}(t)}{\mathrm{d}t} - M_{23} \frac{\mathrm{d}i_{L_3}(t)}{\mathrm{d}t}) \tag{3}$$

- KCL at node 2 yields:

$$0 = -g_m e(t) - i_m(t) + \frac{1}{n} i_p(t) + i_{L_3}(t) + g_{s3}(L_3 \frac{\mathrm{d}i_{L_3}(t)}{\mathrm{d}t} - M_{23} \frac{\mathrm{d}i_{L_2}(t)}{\mathrm{d}t}) \tag{4}$$

- KVL loop: node 1 to transformer to node 2, yields:

$$0 = -v_1(t) + v_2(t) + e(t) + L_1 \frac{\mathrm{d}i_{L_1}(t)}{\mathrm{d}t} + r_1(g_m e(t) + i_m(t) - \frac{1}{n} i_p(t)) \tag{5}$$

- KVL loop: node 3 to node 1, yields:

$$0 = -v_3(t) + v_1(t) + r_2(i_{L_2}(t) + g_{s_2}(L_2 \frac{\mathrm{d}i_{L_2}(t)}{\mathrm{d}t} - M_{23} \frac{\mathrm{d}i_{L_3}(t)}{\mathrm{d}t}) + L_2 \frac{\mathrm{d}i_{L_2}(t)}{\mathrm{d}t} - M_{23} \frac{\mathrm{d}i_{L_3}(t)}{\mathrm{d}t} \tag{6}$$

- KVL loop: node 2 to node 4, yields:

$$0 = -v_2(t) + v_4(t) + r_3(i_{L_3}(t) + g_{s_3}(L_3 \frac{\mathrm{d}i_{L_3}(t)}{\mathrm{d}t} - M_{23} \frac{\mathrm{d}i_{L_2}(t)}{\mathrm{d}t}) + L_3 \frac{\mathrm{d}i_{L3}(t)}{\mathrm{d}t} - M_{23} \frac{\mathrm{d}i_{L_2}(t)}{\mathrm{d}t} \tag{7}$$

- KCL at node 3 yields:

$$0 = i_{L_2}(t) + g_{s2}(L_2 \frac{\mathrm{d}i_{L_2}(t)}{\mathrm{d}t} - M_{23} \frac{\mathrm{d}i_{L_3}(t)}{\mathrm{d}t}) + g_b(v_3(t) - v_4(t)) \tag{8}$$

- KCL at node 4 yields:

$$0 = -i_{L_3}(t) - g_{s3}(L_3 \frac{\mathrm{d}i_{L_3}(t)}{\mathrm{d}t} - M_{23} \frac{\mathrm{d}i_{L_2}(t)}{\mathrm{d}t}) + g_b\,(v_4(t) - v_3(t)) \tag{9}$$

- Transformer magnetizing leg yields:

$$0 = e(t) - \frac{\mathrm{d}\lambda(t)}{\mathrm{d}t} \tag{10}$$

$$0 = y_1(t) - \left(\frac{\lambda(t)}{\lambda_0}\right)^2 \tag{11}$$

$$0 = y_2(t) - (y_1(t))^2 \tag{12}$$

$$0 = y_3(t) - (y_2(t))^2 \tag{13}$$

$$0 = y_4(t) - y_3(t) y_1(t) \tag{14}$$

$$0 = i_m(t) - i_0 \left(\frac{\lambda(t)}{\lambda_0}\right) y_4(t) - \frac{1}{L_0} \lambda(t) \tag{15}$$

3) Derived measurements: This measurements are related with the current $i_b{}^m$ that goes through the burden resistor. This current is not measured but it can be derived, as it is proportional to *Vout*. They respond as well to the physical laws that the instrumentation channel must obey.

$$i_b^m(t) = -g_b(v_3(t) - v_4(t)) \tag{16}$$

$$i_b^m(t) = i_{L_1}(t) + g_{s1}L_1\frac{\mathrm{d}i_{L_1}}{\mathrm{d}t} \tag{17}$$

$$i_b^m(t) = i_{L_2}(t) + g_{s2}\left(L_2\frac{\mathrm{d}i_{L_2}}{\mathrm{d}t} - M_{23}\frac{\mathrm{d}i_{L_3}}{\mathrm{d}t}\right) \tag{18}$$

$$i_b^m(t) = i_{L_3}(t) + g_{s3}\left(L_3\frac{\mathrm{d}i_{L_3}}{\mathrm{d}t} - M_{23}\frac{\mathrm{d}i_{L_2}}{\mathrm{d}t}\right) \tag{19}$$

$$i_b^m(t) = g_m e(t) + i_m(t) - \frac{1}{n}i_p(t) \tag{20}$$

4) Pseudo measurements: This section only include one measurement, the ground voltage, that is difficult to measure. However, it is expected to be close to zero.

$$0^m = v_4(t) \tag{21}$$

Based on this, the vector of measurements, z, whose size is 21-by-1 elements, can be expressed as:

$$z = [V_{out}(t)\ 0\ 0\ 0\ 0\ 0\ 0\ 0\ 0\ 0\ 0\ 0\ 0\ 0\ 0\ 0\ 0\ 0\ 0\ 0\ 0\ I_b^m(t)\ I_b^m(t)\ I_b^m(t)\ I_b^m(t)\ I_b^m(t)\ 0]$$

B. State estimation

Once the mathematical model of the measurements has been derived, it is possible to define the algorithm of state estimation. This algorithm, that is repeated for each sample, can be summarized in the workflow shown in Figure 3.

It consists on an iterative process that improve the estimation for each state variable based on the expected variances associated to each measurement. Therefore, those measurements that are more reliable - have less variance - will be taken more in consideration than others that present a larger variance. The formulation of the algorithm is as follows:

$$x^{v+1} = x^v + (H^T W H)^{-1} H^T W(z - h(x^v)) \tag{22}$$

Where x^{v+1} is the estimated state vector of the next iteration, x^v is the estimated state vector of the current iteration, H is the Jacobian matrix that relates the measurements with the state vector, W is the matrix that gathers the inverse of the variances of all the measurements on the main diagonal, z is the vector of measurements for each sample for a certain moment of time that want to be estimated and $h(x^v)$ is the vector of equations that was used to derive H evaluated for x^v.

The iterative algorithm will stop when the largest difference between the elements of x^{v+1} and x^v is less than 0.0001. This tolerance is set small to ensure that the results of the state estimation are accurate enough, and that more iterations wouldn't give a significant improvement.

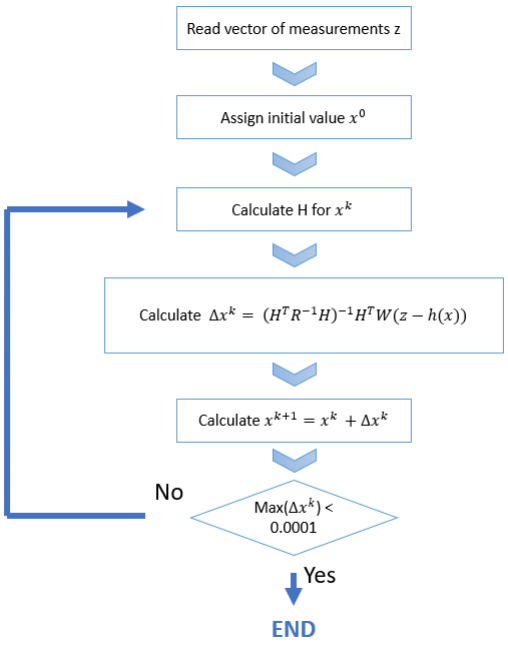

Fig. 3. Workflow of the state estimation algorithm

1) Jacobian matrix: The Jacobian matrix, whose size is 21-by-15, associates the 21 measurements - the rows - with the 15 state variables - the columns. Each element is obtain as the partial derivative of each equation with respect to each state variable. This can be represented as follows:

$$H = \begin{bmatrix} \frac{\partial h_1(x)}{\partial x_1} & \dots & \frac{\partial h_1(x)}{\partial x_{15}} \\ \dots & \dots & \dots \\ \frac{\partial h_{21}(x)}{\partial x_1} & \dots & \frac{\partial h_{21}(x)}{\partial x_{15}} \end{bmatrix} \tag{23}$$

However, some equations includes derivatives of some state variables and therefore all the terms inside those equations need to be integrated prior to the construction of the matrix. The chosen type of the integration is the trapezoidal integration, which has the following form:

- For terms that don't have a derivative:

$$\int_{t-h}^{t} x(\tau)d\tau = \frac{h}{2}(x(t-h) + x(t)) \tag{24}$$

- For terms that have a derivative:

$$\int_{t-h}^{t} \frac{\mathrm{d}x(\tau)}{\mathrm{d}\tau}d\tau = (x(t) - x(t-h)) \tag{25}$$

The equations that need to be integrated are 2, 3, 4, 5, 6, 7, 8, 9, 10, 17, 18 and 19. The integration has to take place on both sides of the equation, clearing the variable at time t in the left side. The integrated equations are shown in the Appendix.

Note that the matrix H doesn't depend on the state on the previous sample - i.e, there are no terms of *(t-h)*. However, there are terms of *(t)*, what means that the matrix H has to be recomputed for each iteration of x^v.

2) W matrix: As it has been mentioned before, the matrix W gathers the inverse of the variances of all the measurements on the main diagonal. Those variances depend on the type of measurements. In this project, as indicated in [1], the standard deviations, σ, are:

TABLE I
STANDARD DEVIATION FOR DIFFERENT TYPES OF MEASUREMENTS

Type of measurement	Standard deviation (σ)
Actual	0.05 %
Virtual	0.005 %
Derived	0.05 %
Pseudo	10 %

Then, the matrix W can be represented as follows:

$$W = diag(\frac{1}{\sigma_1^2}, \frac{1}{\sigma_2^2}, ..., \frac{1}{\sigma_{21}^2}) \tag{26}$$

C. Chi-Square test

Once the state estimation is performed, it is necessary to check that the distribution of measurement errors is reasonable. This is accomplished with the Chi-Square test. Before explaining how the test works, a few concepts have to be introduced.

The normalized error s_i - also called normalized residual - for each measurement z_i is calculated as follows:

$$s_i = \frac{z_i - h_i(x^v)}{\sigma_i^2} \tag{27}$$

The Chi-Square variable for the state estimation, χ^2, is computed as it is detailed next:

$$\zeta = \chi^2 = \sum_{i=1}^{21} s_i^2 \tag{28}$$

Where ζ is the sum of squares of the normalized residuals.The probability distribution of the Chi-Square variable, for a certain number of degrees of freedom ν, is:

$$Pr(\zeta, \nu) = Pr[x^2 \leq \zeta] \tag{29}$$

Note that this formulation of the probability distribution returns a larger value for a larger ζ. The larger the summation of residuals, the easiest the variable x^2 is lower than $\zeta = \chi^2$. This is related with them concept of critical value: If ζ is too large, that means that the errors are not reasonable.

The number of degrees of freedom is the difference between the number of measurements and the number of state variables. Therefore, the number of degrees of freedom is $\nu = 21 - 15 = 6$. In Figure 4, the probability distributions for several degrees of freedom are shown.

For a given number of degrees of freedom, the larger ζ, the larger probability that the error is outside the reasonable bounds. The goodness of fit is measured in the following way:

$$Pr[\chi^2 \geq \zeta] = 1 - Pr[\chi^2 \leq \zeta] = 1 - P(\zeta, \nu) \tag{30}$$

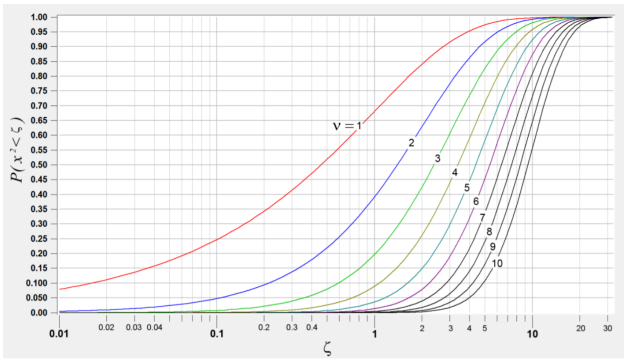

Fig. 4. Probability distribution of χ^2 for several degrees of freedom

This measure, $Pr[\chi^2 \geq \zeta]$, is called P-value. Therefore, if the summation of squares of the normalized residuals is small, then the P-value will be near 1, and the measurement errors will be considered as reasonable. The larger the error, the closer the P-value will be close to 0. This leads to the concept of confidence level, which is the maximum deviation from 1 that is considered as acceptable. The confidence level is set to 0.1, so if the goodness of fit returns a P-value lower than 0.9 the algorithm will determine that a fault in the system has occurred.

D. User Interface

This graphical user interface (GUI) has been developed with MATLAB AppDesigner. The functionalities of this application are to read recorded data in COMTRADE format - which includes some recording parameters in a .cfg file and the actual data in a .dat file -, the state estimation based on the given measurements and the visualization of some interesting plots that will help to analyze the estimation. The documentation about the COMTRADE format was accessed at [2]. Additionally, if there is a fault during the recorded data, the GUI will display the exact moment of the fault occurrence.

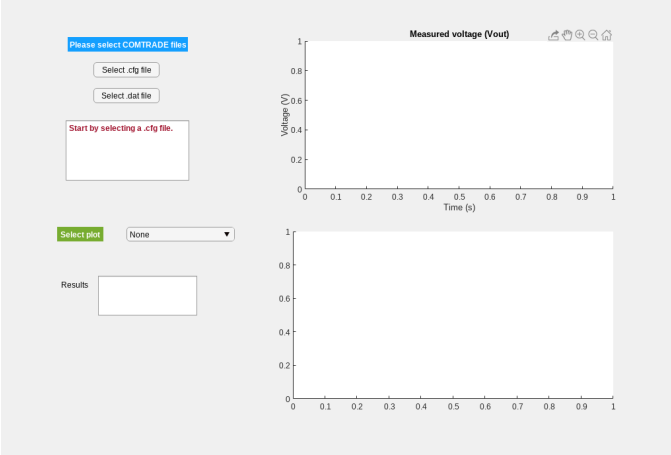

Fig. 5. First screen of the application

In Figure 5, the first screen of the application is shown. The message displayed on the text box - "Start by selecting a

.cfg file" - invites the user to browse the file that contains the parameters in first place.

Once the file is loaded, a new message request the loading of the .dat file that contains the recorded measurements, as it can be seen in Figure 6. The message states: "Now select a .dat file. Later, please wait a few seconds until the state estimation is performed." Once the file is uploaded, the algorithm that runs the application will start performing the state estimation. The application won't show any new output until this step is completed.

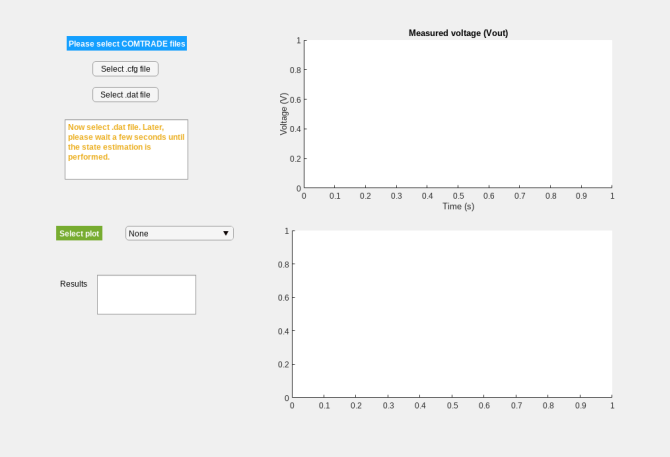

Fig. 6. Application request for .dat file

A few seconds later, the application will update the shown message, that will change to "State estimation completed. Results are available below. Proceed to select plot." This message can be appreciated on Figure 7.

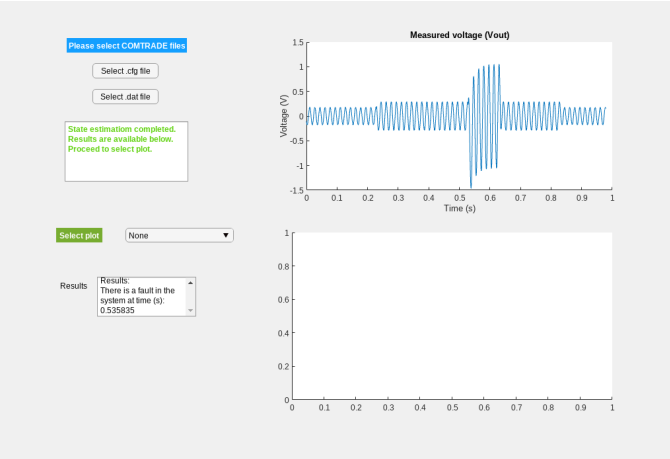

Fig. 7. Application outputs update after state estimation

On the upper plot, the recorded voltage measurements will be displayed after the conversion applied to the COMTRADE format has ended. Therefore, the real magnitude of the voltage waveform is displayed. The "Results" text box will inform the user about whether a fault has occurred during the recorded measurements or not. If the result is positive, the precise moment when this fault occurred, according to the state estimation results, will be displayed at the end of the message: "There is a fault in the system at time (s): ." If the result is negative, on the contrary, the message will be: "There is no fault in the system."

Finally, the application gives the user a selection of plots that gathers the most relevant magnitudes and information, so the user can extract insights of the system behaviour. The available plots are:

- Estimated Ip.
- Difference between Ip and CT*Ib.
- Linkage flux.
- Chi Square test.
- Residuals.

IV. Results

In this section, the two events given for the projects will be analyzed using the plots given by the GUI. The presence of a fault will be also discussed.

A. Event 01

The GUI shows that there is a fault at time 0.535 seconds, as it can be appreciated in Figure 8. Taking a look at the result of the Chi-Square test along all the event, there is a drop at that moment of time in which the P-value is approximately 0.6, which is clearly below the threshold of 0.9 that correspond to a level of confidence of 0.1. This low results comes from the fact that the fault introduces unexpected measurements that doesn't fit or resemble what would be expected given the model definition of the system.

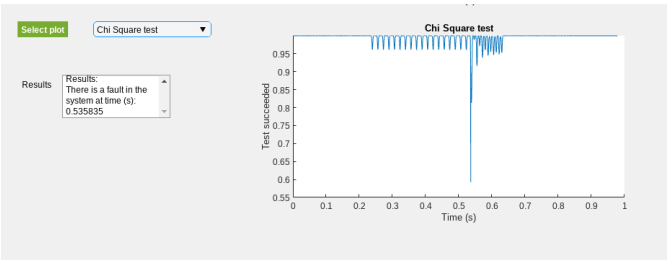

Fig. 8. Results and Chi-Square test for the state estimation of Event 01

In Figure 9, the estimated primary current is shown. The waveform is similar to the measured output voltage.

However, it is more interesting to look at the difference between the estimated primary current and the secondary current times the transformation ratio - CTI_b. In Figure 10, it is possible to see that the difference is very close to 0 Amperes before the fault, which is negligible in comparison to the magnitudes of the current, but after the fault increases to a maximum difference of about 2.5 A. Even when the fault is cleared, the difference between the currents never go back to 0 A, instead it remains stable about 1.5 A.

The fact that there is a difference between I_p and $CT\ I_b$ reinforces the importance of performing this state estimation to know exactly which is the current flowing through the line.

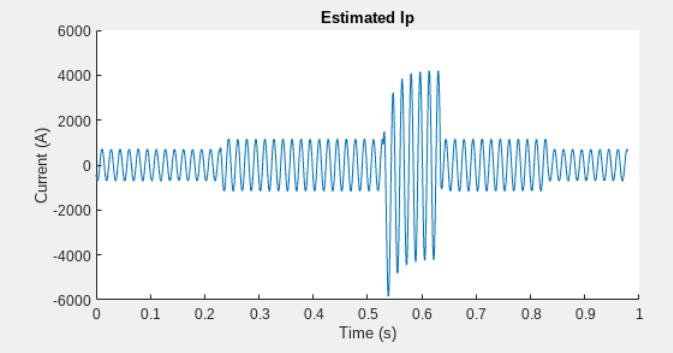

Fig. 9. Estimated primary current for Event 01

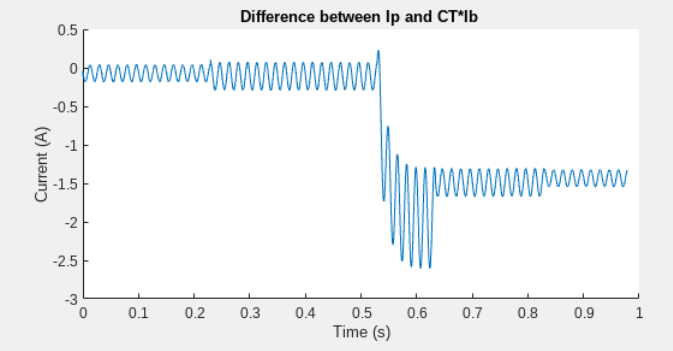

Fig. 10. Difference between estimated I_p and $CT\ I_b$ for Event 01

The reason behind this sudden increase of difference in the moment of the fault is that the saturation of the core has an effect on the amount of current that is induced on the secondary side of the transformer. Therefore, the secondary current is not reflecting properly the current that goes through the line. In this case, the difference is not crucial, but in other instrumentation channels or in other situations it could be.

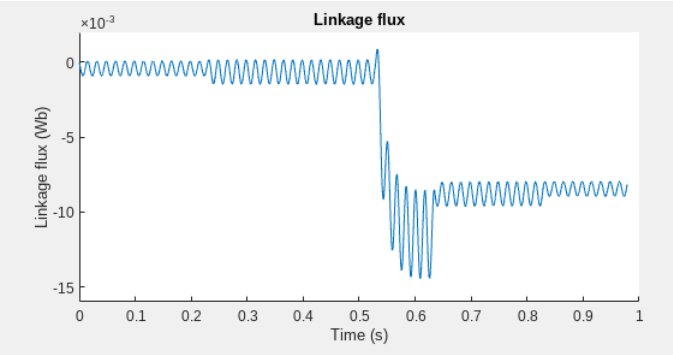

Fig. 11. Linkage flux across the magnetic core for Event 01

In Figure 11, the linkage flux across the magnetic core is displayed. The waveform resembles the difference shown in Figure 10, which is not surprising as both are related with the magnetizing branch. There is an increase in the magnitude of the flux at the moment of the fault, what it is related with the fact that during the fault the current that goes through the line is larger, inducing then a larger flux.

A interesting plot to see is the evolution of the value of the individual residuals along the time, included in Figure 12. Larger residuals are always associated to measurements 4, 9 and 11, which are KCL at node 2, KCL at node 4 and the equation that relates $y_1\ (t)$ and $\lambda(t)$, respectively. This last measurement is significantly larger just in the moment of the fault. However, just after the fault, it has much less magnitude than the other two residuals. These larger residuals mean that the variations in those measurements are much larger than expected.

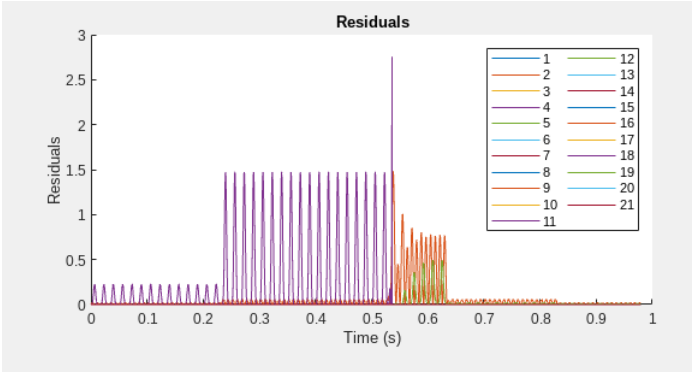

Fig. 12. Residuals for Event 01

B. Event 02

An analysis similar to the one performed for Event 01 is performed for Event 02. In Figure 13, the screen shown is just after the state estimation is finished. The upper plot shows the measured output voltage. The ”Results” text box displays that a fault occurred at 0.530 seconds.

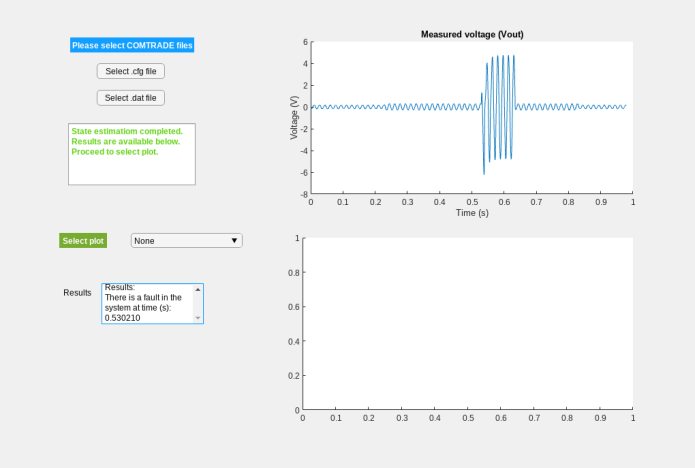

Fig. 13. Screen after the state estimation is completed for Event 02

Looking at the results of the Chi-Square test in Figure 14 it is possible to notice that in the second event the P-value touches zero several times, instead of dropping just once below

the threshold of 0.9 as in the previous event. This is reasonable taking in account the relative difference of output voltage in Event 02 between when there is no fault and the moment of the fault is much larger than in Event 01.

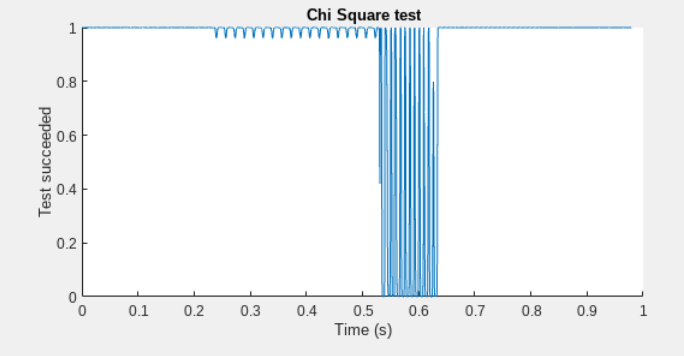

Fig. 14. Results and Chi-Square test for the state estimation of Event 02

The estimated primary current for Event 02, shown in Figure 15, reflects as well that larger relative change between the current that flows through the line during the normal operation and during the fault.

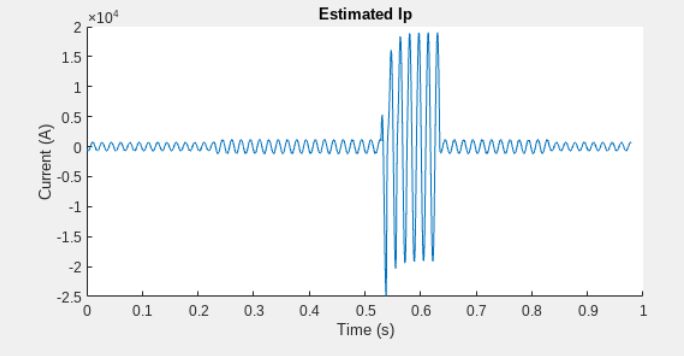

Fig. 15. Estimated primary current for Event 02

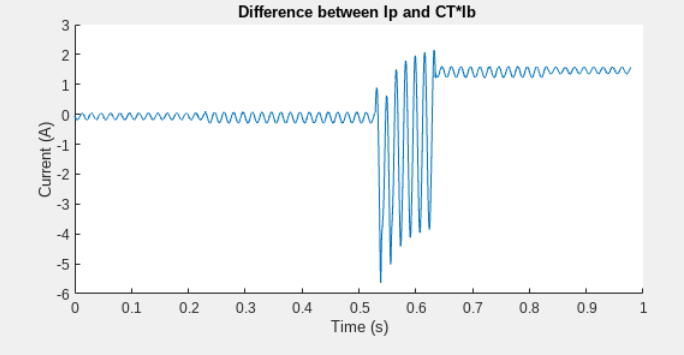

Fig. 16. Difference between estimated I_p and CTI_b for Event 02

In Figure 16, it is plotted the difference between the estimated I_p and $CT\ I_b$. The difference is very close to zero before the fault. During the fault the peak goes up to 5 Amperes of difference. After the fault is cleared, the difference goes around 1 A, which is almost negligible in comparison to the magnitude of the currents.

As happened for Event 01, the magnitude of the difference between those two currents is larger just after the fault. This fact is related with the saturation of the transformer during that time.

The linkage flux, shown in Figure 17, has as well a similar waveform to the difference of currents shown before. The increase of the flux is explained because of the increment of the primary current, as it also happened in the Event 01. It is also noticeable that for the second event, the flux tends to increase after the fault, while in the first event it tends to decrease.

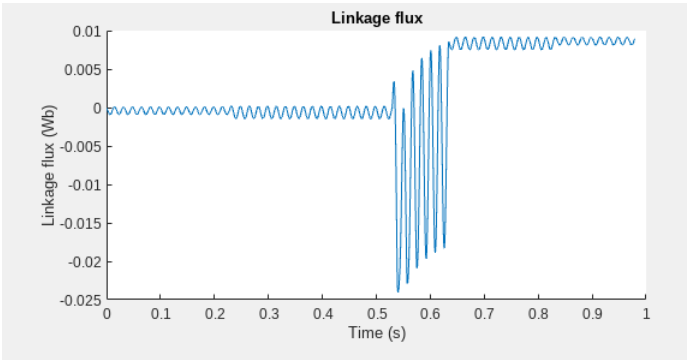

Fig. 17. Linkage flux across the magnetic core for Event 02

The analysis of the residuals that can be appreciated in Figure 18 for the second event draws conclusions similar to Event 01. The larger residuals are always associated to measurements 4, 9 and 11. The residuals have a larger magnitude than for Event 01 during the fault, what explains why the Chi-Square test fails more.

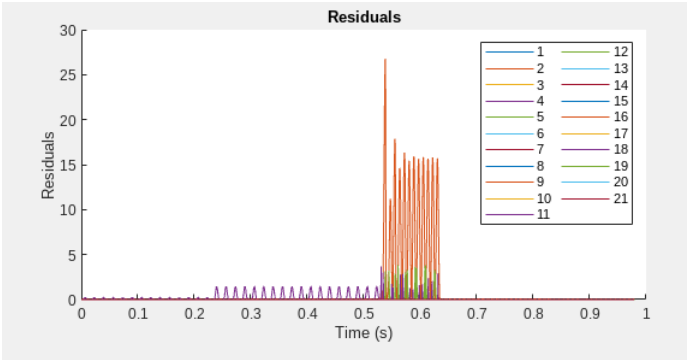

Fig. 18. Residuals for Event 02

V. Conclusions

This project aimed to develop a state estimation method for a current instrumentation channel in order to detect a fault in the system. A graphical user interface (GUI) has been developed to facilitate the analysis of the system and display useful information.

The detection of a fault depends on the measurements of the current that flows through the line. It is known than the saturation of the transformer of the instrumentation channel could lead to incorrect measurements during a fault. The state estimation approach tries to mitigate the effect of saturation and it do show that, specially during the fault, there is a difference between the estimated primary current and the secondary current times the current ratio of the transformer - that would be what the relay would measure if this state estimation wasn't performed. However, this difference for both events in negligible in comparison to the actual magnitude of the currents.

In order to detect if a fault has occurred in the system, the algorithm uses the Chi-Square test to validate the results of the state estimation. If the confidence of the estimation is below a threshold, that means that the estimation doesn't fit with what should be expected - the state of the system has changed too fast. This implies that a fault has occurred. According to this criteria, there is a fault in both events. In the second event, the confidence of the estimation is remarkably lower than in the first event. This is related with the fact that the relative increase of the current during the fault in the second event is larger than during the first event.

Additionally, the linkage flux waveform and its similarity to the difference between I_p and $CT\ I_b$ has been discussed. The analysis of the residuals along the time draws interesting conclusions: the measurements with larger residuals are KCL at node 2, KCL at node 4 and the equation that relates $y_1\ (t)$ and the linkage flux, $\lambda(t)$. The residuals in the second event are larger during the fault and therefore, the confidence of the estimation returned by the Chi-Square test is much lower than in the first event.

REFERENCES

[1] A.P. Meliopoulos, Fellow, IEEE, George Cokkinides, Member, IEEE, Jiahao Xie and Yuan Kong, "Instrumentation Error Correction within Merging Units" School of Electrical and Computer Engineering, Georgia Institute of Technology, Atlanta, GA, U.S.A.

[2] IEEE Standard Common Format for Transient Data Exchange (COMTRADE) for Power Systems," in IEEE Std C37.111-1999 , vol., no., pp.1-55, 15 Oct. 1999

APPENDIX

List of model parameters:

Parameter	Value
n	400
g_m	0.001 S
L_1	26.526 µH
L_2	348.0 µH
L_3	348.0 µH
M_{23}	287.0 µH
g_{s1}	1.9635 S
g_{s2}	0.1497 S
g_{s3}	0.1497 S
r_1	0.005 Ω
r_2	0.4469 Ω
r_3	0.4469 Ω
R_b	0.1 S
λ_0	0.1876 Wb
i_0	6.09109 A
L_0	2.36 H

Equations 2 to 10 after trapezoidal integration:

$$0 = -g_m\frac{h}{2}(e(t-h)+e(t)) - \frac{h}{2}(i_m(t-h)+ i_m(t)) + \frac{h}{2n}(i_p(t-h)+i_p(t)) + \frac{h}{2}(i_{L_1}(t-h)+ i_{L_1}(t)) + g_{s1}L_1(i_{L_1}(t) - i_{L_1}(t-h)$$

$$0 = -g_m\frac{h}{2}(e(t-h)+e(t)) - \frac{h}{2}(i_m(t-h)+i_m(t))+ \frac{h}{2n}(i_p(t-h)+i_p(t)) + \frac{h}{2}(i_{L_1}(t-h)+ i_{L_1}(t)) + g_{s1}L_1(i_{L_1}(t) - i_{L_1}(t-h)$$

$$0 = g_m\frac{h}{2}(e(t-h)+e(t)) + \frac{h}{2}(i_m(t-h)+i_m(t))- \frac{h}{2n}(i_p(t-h)+i_p(t)) - \frac{h}{2}(i_{L_2}(t-h)+i_{L_2}(t))- g_{s2}L_2(i_{L_2}(t) - i_{L_2}(t-h) + g_{s2}M_{23}(i_{L_3}(t) - i_{L_3}(t-h)$$

$$0 = -g_m\frac{h}{2}(e(t-h)+e(t)) - \frac{h}{2}(i_m(t-h)+i_m(t))+ \frac{h}{2n}(i_p(t-h)+i_p(t)) + \frac{h}{2}(i_{L_3}(t-h)+i_{L_3}(t))+ g_{s3}L_3(i_{L_3}(t) - i_{L_3}(t-h) - g_{s3}M_{23}(i_{L_2}(t-h)+i_{L_2}(t))$$

$$0 = -\frac{h}{2}(v_1(t-h)+v_1(t)) + \frac{h}{2}(v_2(t-h)+v_2(t))+ \frac{h}{2}(e(t-h)+e(t)) + L_1(i_{L_1}(t) - i_{L_1}(t-h))+ r_1g_m\frac{h}{2}(e(t-h)+e(t)) + r_1\frac{h}{2}(i_m(t)+i_m(t-h))- \frac{r_1h}{2n}(i_p(t-h)+i_p(t))$$

$$0 = -\frac{h}{2}(v_3(t-h)+v_3(t)) + \frac{h}{2}(v_1(t-h)+v_1(t))+ \frac{r_1h}{2}(i_{L_2}(t)+i_{L_2}(t-h)) + r_2g_{s2}L_2(i_{L_2}(t) - i_{L_2}(t-h))- r_2g_{s2}M_{23}(i_{L_3}(t) - i_{L_3}(t-h)) + L_2(i_{L_2}(t)- i_{L_2}(t-h)) - M_{23}(i_{L_3}(t) - i_{L_3}(t-h))$$

$$0 = -\frac{h}{2}(v_2(t-h)+v_2(t)) + \frac{h}{2}(v_4(t-h)+v_4(t))+ \frac{r_3h}{2}(i_{L_3}(t)+i_{L_3}(t-h)) + r_3g_{s3}L_3(i_{L_3}(t) - i_{L_3}(t-h))- r_3g_{s3}M_{23}(i_{L_2}(t) - i_{L_2}(t-h)) + L_3(i_{L_3}(t) - i_{L_3}(t-h))- M_{23}(i_{L_2}(t) - i_{L_2}(t-h))$$

$$0 = \frac{h}{2}(i_{L_2}(t)+i_{L_2}(t-h)) + g_{s2}L_2(i_{L_2}(t)- i_{L_2}(t-h)) - g_{s2}M_{23}(i_{L_3}(t) - i_{L_3}(t-h))+ \frac{g_bh}{2}(v_3(t-h)+v_3(t)) - \frac{g_bh}{2}(v_4(t-h)+v_4(t))$$

$$0 = -\frac{h}{2}(i_{L_3}(t) + i_{L_3}(t-h)) - g_{s3}L_3(i_{L_3}(t) - i_{L_3}(t-h)) + g_{s3}M_{23}(i_{L_2}(t) - i_{L_2}(t-h)) + \frac{g_b h}{2}(v_4(t-h) + v_4(t)) - \frac{g_b h}{2}(v_3(t-h) + v_3(t))$$

$$0 = \frac{h}{2}(e(t-h) + e(t)) - (\lambda(t) - \lambda(t-h))$$

Equations 17 to 20 after trapezoidal integration:

$$i_b^m(t) = \frac{2}{h}(\frac{h}{2}(i_{L_1}(t) + i_{L_1}(t-h)) + g_{s1}L_1(i_{L_1}(t) - i_{L_1}(t-h))) - i_b^m(t-h)$$

$$i_b^m(t) = \frac{2}{h}(\frac{h}{2}(i_{L_2}(t) + i_{L_2}(t-h)) + g_{s2}L_2(i_{L_2}(t) - i_{L_2}(t-h)) - g_{s2}M_{23}(i_{L_3}(t) - i_{L_3}(t-h))) - i_b^m(t-h)$$

$$i_b^m(t) = \frac{2}{h}(-\frac{h}{2}(i_{L_3}(t) + i_{L_3}(t-h)) - g_{s3}L_3(i_{L_3}(t) - i_{L_3}(t-h)) + g_{s3}M_{23}(i_{L_2}(t) - i_{L_2}(t-h))) - i_b^m(t-h)$$